Original Article

pISSN 2234-7518 • eISSN 2005-372X
http://dx.doi.org/10.4041/kjod.2013.43.2.62

THE KOREAN JOURNAL of ORTHODONTICS
KJO

New three-dimensional cephalometric analyses among adults with a skeletal Class I pattern and normal occlusion

Mohamed Bayome[a]
Jae Hyun Park[b,c]
Yoon-Ah Kook[d]

[a]Graduate School, The Catholic University of Korea, Seoul, Korea
[b]Postgraduate Orthodontic Program, Arizona School of Dentistry and Oral Health, A.T. Still University, Mesa, AZ, USA
[c]Graduate School of Dentistry, Kyung Hee University, Seoul, Korea
[d]Department of Orthodontics, Seoul St. Mary's Hospital, The Catholic University of Korea, Seoul, Korea

Objective: The purpose of this study was to assess new three-dimensional (3D) cephalometric variables, and to evaluate the relationships among skeletal and dentoalveolar variables through 3D cephalometric analysis. **Methods:** Cone-beam computed tomography (CBCT) scans were acquired from 38 young adults (18 men and 20 women; 22.6 ± 3.2 years) with normal occlusion. Thirty-five landmarks were digitized on the 3D-rendered views. Several measurements were obtained for selected landmarks. Correlations among different variables were calculated by means of Pearson's correlation coefficient values. **Results:** The body of the mandible had a longer curve length in men (102.3 ± 4.4 mm) than in women (94.5 ± 4.7 mm) ($p < 0.001$), but there was no significant difference in the maxillary basal curve length. Men had significantly larger facial dimensions, whereas women had a larger gonial angle (117.0 ± 4.0 vs. 113.8 ± 3.3; $p < 0.001$). Strong-to-moderate correlation values were found among the vertical and transverse variables ($r = 0.71$ to 0.51). **Conclusions:** The normative values of new 3D cephalometric parameters, including the maxillary and mandibular curve length, were obtained. Strong-to-moderate correlation values were found among several vertical and transverse variables through 3D cephalometric analysis. This method of cephalometric analyses can be useful in diagnosis and treatment planning for patients with dentofacial deformities.
[Korean J Orthod 2013;43(2):62-73]

Key words: Three-dimensional cephalometrics, Three-dimensional diagnosis and treatment planning, Ethnic norms, Anatomy

Received July 24, 2012; Revised December 31, 2012; Accepted January 2, 2013.

Corresponding author: Yoon-Ah Kook.
Professor, Department of Orthodontics, Seoul St. Mary's Hospital, The Catholic University of Korea, 222 Banpo-daero, Seocho-gu, Seoul 137-701, Korea.
Tel +82-2-2258-1776 e-mail kook190036@yahoo.com

*This study was partially supported by the Alumni Fund of the Department of Dentistry and Graduate School of Clinical Dental Science, The Catholic University of Korea

The authors report no commercial, proprietary, or financial interest in the products or companies described in this article.

INTRODUCTION

Cephalometric analysis has been a key element in diagnosis and treatment planning for orthodontic and orthognathic surgery patients. However, errors in identification of landmarks, their projection in two dimensions, superimposition of anatomical structures, and implications relative to head orientation have raised questions about the reliability of the analyses.[1,2] Therefore, several methods have been attempted to achieve a three-dimensional (3D) evaluation from the two-dimensional (2D) cephalographs.[3-5]

Recently, several advantages of cone-beam computed tomography (CBCT) have been reported, including the ability to assess an image from the three planes, the ability to obtain life-sized 3D images, and the lack of distortion or overlapping structures.[6] Moreover, it is not essential to make a fine adjustment of head position during imaging and analysis, because the points maintain their spatial relationships.[7] Some authors have reported ease of landmark identification and high precision of superimposing images with CBCT.[8,9]

van Vlijmen et al.[10,11] have reported clinically relevant differences between angular measurements taken from 2D postero-anterior cephalographs and those from radiographs or 3D models constructed from CBCT scans. Gribel et al.[12] concluded that measurements taken from a conventional lateral cephalogram were significantly different than those taken from a CBCT scan of the same person. Therefore, they presented a mathematical formula to enable the correction of 2D into 3D CBCT measurements.

Several investigators have attempted to develop 3D analyses to cope with the huge amount of information provided by the 3D technologies. Farronato et al.[13] proposed a 10-point 3D analysis of CBCT images directly digitized on the rendered view. They evaluated the reliability and reproducibility of their method and compared their results to 2D data. However, norms of the variables were not reported in their study, probably because of the small sample size and wide range in age. Cheung et al.[14] reported 3D cephalometric norms on the basis of CBCT scans from a Chinese population. However, there was no assessment of the relationships among the cephalometric variables and no attempt to evaluate the curved nature of the mandible and maxilla. The aims of this study were to assess new 3D cephalometric variables from a normal occlusion sample and to evaluate the relationships among skeletal and dentoalveolar variables through a 3D cephalometric analysis.

MATERIALS AND METHODS

Thirty-eight Korean young adults (18 men and 20 women; 22.6 ± 3.2 years) with normal occlusion were recruited from the College of Dentistry, Wonkwang University (Iksan, Korea), and the Nursing School, The Catholic University of Korea (Seoul, Korea). Approval for this study was obtained from the Institutional Review Board of The Catholic University of Korea, Catholic Clinical Research Coordinating Center (IRB No. KC11EASE0182), and informed consent was obtained according to the Declaration of Helsinki.

The inclusion criteria were as follows: 1. Balanced facial appearance decided by agreement of 2 independent orthodontists; 2. Class I skeletal relationship; 3. Class I molar and canine relationship; 4. Full permanent dentition with the exception of the 3rd molars; 5. 1- to 3-mm arch length discrepancy in each jaw; 6. Normal curve of Spee of 0 to 2 mm; 7. Absence of dental rotation; 8. Coincidental facial and dental midlines; 9. Absence of extensive restorations involving the proximal areas or the labial surfaces; 10. No previous orthodontic treatment; and 11. No acute or previous temporomandibular disorder.

The CBCT scans were acquired with an Alphard 3030 (Asahi Roentgen Ind. Co. Ltd., Kyoto, Japan) machine. Subjects were positioned such that the soft-tissue contours of their faces were included in the scan. The following settings were applied: 80 kV; 5.00 mA; field of view, 200 × 179 mm; exposure time, 17 s; and voxel size, 0.39 mm. The voxels were exported in the digital imaging and communications in medicine (DICOM) format. Invivo 5.1 (Anatomage, San Jose, CA, USA) software was used to reconstruct the voxels, view, digitize, and measure the CBCT scans. First, reorientation

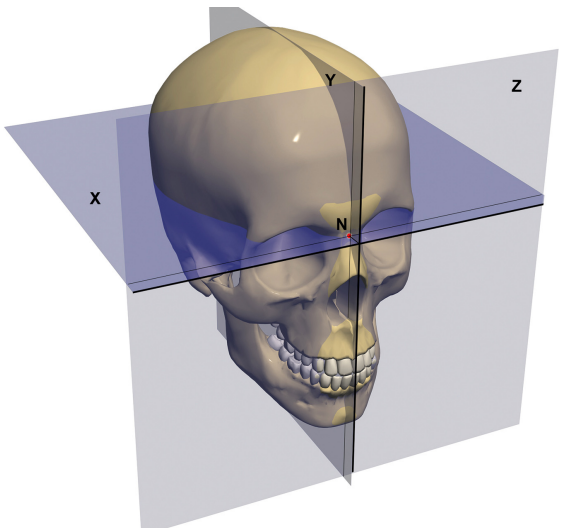

Figure 1. Reorientation of head and coordinate system. N, Nasion; X, the horizontal plane; Y, the midsagittal plane; Z, the vertical plane.

 http://dx.doi.org/10.4041/kjod.2013.43.2.62

of the head position of each scan was performed. Nasion (N) was selected as the origin of the X, Y, and Z coordinates. The horizontal plane (X) was the plane passing through N and parallel to the plane defined through the right and left orbitales (Or) and the left porion (Po), while the midsagittal plane (Y) was defined as the perpendicular plane passing through the origin N and anterior nasal spines (ANS). The vertical plane (Z) was perpendicular to both X and Y passing through N (Figure 1).

Table 1 shows the definition of the hard- and soft-tissue landmarks digitized on the 3D-rendered view of the images. The software calculated the linear and angular dimensions between certain landmarks, according to the definitions given in Figures 2 - 5 and Table 2.

To calculate the mandibular body curve (MBC) length, the coordinates of the menton (Me) and the right and left gonion (Go) and MBC points, which lie on the most convex point on the curvature of the mandibular body midway between the inner and outer borders (Figure 5), were entered into a mathematical software (MATLAB® 7.5 [R2007b]; The MathWorks Inc., Natick, MA, USA). Each set of data was translated to position the Me in the origin point. Then, the set was rotated around the X-axis until the Z coordinate of the Go was nullified. The 4th-degree polynomial equation *f(x)* of the best fitting curve that passed through the 5 points was generated as an approximation of the curvature of the mandibular body.

Table 1. Definitions of the three-dimensional skeletal and dentoalveolar landmarks

Landmark	Definition
Cranium	
Nasion (N)	The junction between the nasal and frontonasal sutures
Sella (S)	The center of the sella turcica on the midsagittal plane
Porion (Po)	The most superior point on the upper rim of the external auditory meatus
Orbitale (Or)	The most inferior point on the lower rim of the orbit
Zygomatic point (Z)	The point on orbital rim showing the frontozygomatic suture
Maxilla	
Anterior nasal spine (ANS)	The most anterior point on the floor of nose
Posterior nasal spine (PNS)	The most posterior point on the floor of nose
Maxillary point (M)	The center of the concavity of the zygomatic process of the maxilla
A point (A)	The deepest point between ANS and prosthion at the midsagittal plane
Maxillary tuberosity (Max. T)	The most inferior and lateral point on the maxillary tuberosity
Canine eminence (CE)	The point on the surface of the maxilla corresponding to the canine root apex
Maxillary 1st molar (U6)	Mesiobuccal cusp of the upper 1st molar
Mandible	
B point (B)	The deepest point between pogonion and the alveolus of the lower incisors on the midsagittal plane
Pogonion (Pg)	The most forward-projecting point on the anterior margin of symphysis menti on the midsagittal plane
Gnathion (Gn)	The most inferior point anterior on the anterior margin of symphysis menti on the midsagittal plane
Menton (Me)	The lowermost point on the symphysis menti on the midsagittal plane
Mandibular body curve (MBC)	The most convex point on the curvature, midway between the inner and outer borders of the mandibular body
Gonion (Go)	The midway between the lowermost point on the posterior border of the ramus and the most posterior point on the lower border of the mandible
Sigmoid notch (Sig)	The deepest point on the sigmoid notch
Condylion (Co)	The uppermost point at the center of the condyle
Lateral condyle (Lat Co)	The most lateral point on the mandibular condyle
Medial condyle (Med Co)	The most medial point on the mandibular condyle

http://dx.doi.org/10.4041/kjod.2013.43.2.62

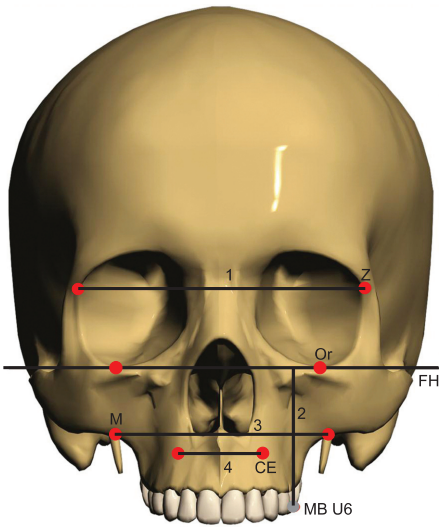

Figure 2. Frontal view shows maxillary landmarks and variables: Z, Zygomatic point; Or, orbitale; FH, Frankfort horizontal plane; M, maxillary point; CE, canine eminence; MB U6, mesiobuccal cusp of upper 1st molar; 1, upper facial width; 2, maxillary height; 3, posterior maxillary basal width; 4, anterior maxillary basal width.

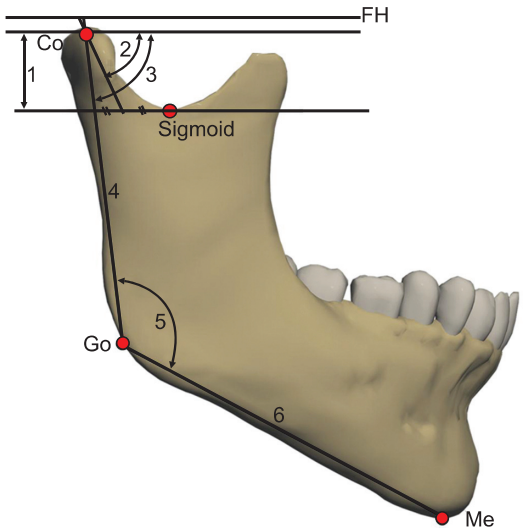

Figure 3. Lateral view of the mandible shows ramal and condylar landmarks and parameters: FH, Frankfort horizontal plane; Co, condylion; Go, gonion; Me, menton; 1, condylar height; 2, condylar anteroposterior inclination; 3, ramal anteroposterior inclination; 4, ramal length; 5, gonial angle; 6, mandibular body length.

$$f(x) = p_1x^4 + p_2x^3 + p_3x^2 + p_4x + ps \quad (1)$$

It was found that the polynomial of the 4th order approximated the curvature of the mandibular body with tolerable, or even negligible, mean square error.

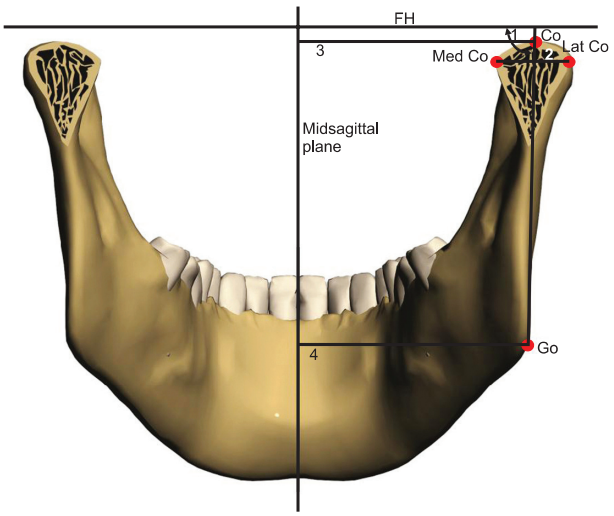

Figure 4. Posterior view of the mandible shows ramal and condylar landmarks and parameters: FH, Frankfort horizontal plane; Co, condylion; Med Co, medial condyle; Lat Co, lateral condyle; Go, gonion; 1, ramal mediolateral inclination; 2, condylar width; 3, condyle to midsagittal plane; 4, gonion to midsagittal plane.

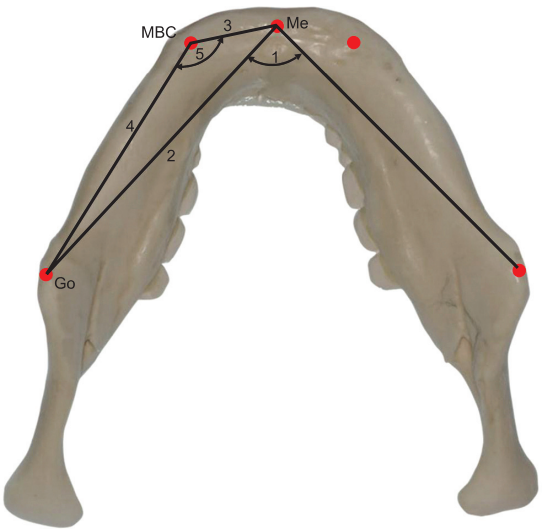

Figure 5. Mandibular body variables: Me, menton; MBC, mandibular body curve; Go, gonion; 1, menton angle; 2, mandibular body length; 3, anterior mandibular body length; 4, posterior mandibular body length; 5, MBC angle.

Mathematically, the length of a path from point *a* to point *b* on a curve represented by the function *f(x)* is given as follows:

$$Length = \int_a^b \sqrt{1 + \left(\frac{df(x)}{dx}\right)^2}\, dx \quad (2)$$

 http://dx.doi.org/10.4041/kjod.2013.43.2.62

Table 2. Definitions of the three-dimensional measurements

Measurement	Definition
Sagittal	
SNA (°)	The angle between the 3 points: S, N, and A, on the midsagittal plane
SNB (°)	The angle between the 3 points: S, N, and B, on the midsagittal plane
ANB (°)	The angle between the 3 points: A, N, and B, on the midsagittal plane
SNPg angle (°)	The angle between the 3 points: S, N, and Pg, on the midsagittal plane
Facial angle (°)	The angle formed by intersection between the N-Pg line and Frankfort horizontal (FH) plane projected on the midsagittal plane
A to N-Pg (mm)	The perpendicular distance from A to N-Pg
Pg to NB (mm)	The perpendicular distance from Pg to N-B
Angle of convexity (°)	The angle between the 3 points: N, A, and Pg, on the midsagittal plane
Maxillary length (mm)	The distance between ANS and PNS
mandibular body length (mm)	The distance between Go and Me
Ramal anteroposterior inclination (°)	The inner angle between Co-Go and the FH plane projected on the midsagittal plane
Condylar anteroposterior inclination (°)	The angle between the vector passing through the Co parallel to the condylar neck, and the FH plane, projected on the midsagittal plane
Vertical	
Anterior facial height (mm)	The vertical distance between N and Me
Upper facial height (mm)	The vertical distance between N and ANS
Lower facial height (mm)	The vertical distance between ANS and Me
Maxillary height (mm)	The perpendicular distance from MB cusp of U6 to the FH plane
Ramal length (mm)	The distance between ipsilateral Co and Go
Condylar height (mm)	The vertical distance from Co to the plane parallel to FH containing the ipsilateral Sig
Y-Axis (°)	The angle formed by intersection between the S-Gn line and FH plane projected on the midsagittal plane
Gonial angle (°)	The angle between the 3 points Me, Go, and Co
Transverse	
Upper facial width (mm)	The horizontal distance between the right and left Z points
Anterior maxillary basal width (mm)	The distance between the right and left CE
Posterior maxillary basal width (mm)	The distance between the right and left M
Me angle (°)	The angle between the right and left Go-Me
Me deviation angle (°)	The angle between the midsagittal plane and the Me-ANS projected on frontal plane
Me to midsagittal (mm)	The perpendicular distance from Me to the midsagittal plane
Ramal mediolateral inclination (°)	The inner angle between Co-Go and the FH plane projected on the frontal plane
Go to midsagittal (mm)	The perpendicular distance from Go to the midsagittal plane
Co to midsagittal (mm)	The perpendicular distance from Co to the midsagittal plane
Condylar width (mm)	The distance between the most medial and lateral points on the condyle head
Other	
Maxillary basal curve length (mm)	The length of the 4th degree polynomial curve from point A, to tuberosity passing through CE
Mandibular basal curve length (mm)	The length of the 4th degree polynomial curve from Me, to Go passing through MBC
MBC angle (°)	The angle formed by the 3 points Me, MBC, and the ipsilateral Go
Anterior mandibular basal length (mm)	The distance between Me and MBC
Posterior mandibular basal length (mm)	The distance between ipsilateral MBC and Go

S, Sella; N, nasion; A, A point; B, B point; Pg, pogonion; ANS, anterior nasal spine; PNS, posterior nasal spine; Go, gonion; Me, menton; Co, condylion; FH, Frankfort horizontal plane; Me, menton; MB, mesiobuccal; U6, upper first molar; Sig, sigmoid notch; Gn, gnathion; Z, zygomamtic point; CE, canine eminence; M, maxillary point; MBC, mandibular body curve.

http://dx.doi.org/10.4041/kjod.2013.43.2.62

Then, the equation was entered into Maple™ 11.0 (Waterloo Maple Inc., Waterloo, ON, Canada) software to calculate the differentiation of the function *f(x)*:

$$\frac{df(x)}{dx} = 4p_1x^3 + 3p_2x^2 + 2p_3x + p_4 \quad (3)$$

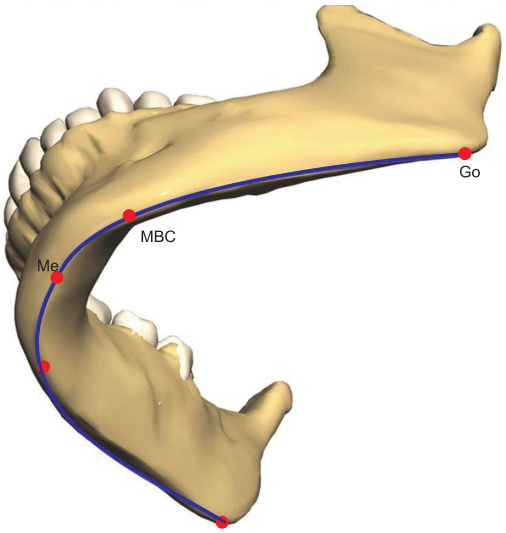

Figure 6. Mandibular basal curve length: Go, gonion; Me, menton; MBC, mandibular body curve.

Then, the length of the curve from Go to Me was found by solving the integration:

$$Length = \int_a^b \sqrt{1 + (4p_1x^3 + 3p_2x^2 + 2p_3x + p_4)^2}\, dx \quad (4)$$

Where *a* and *b* are the values of X coordinates of Me and Go, respectively (Figure 6).

The same procedures were followed to calculate the

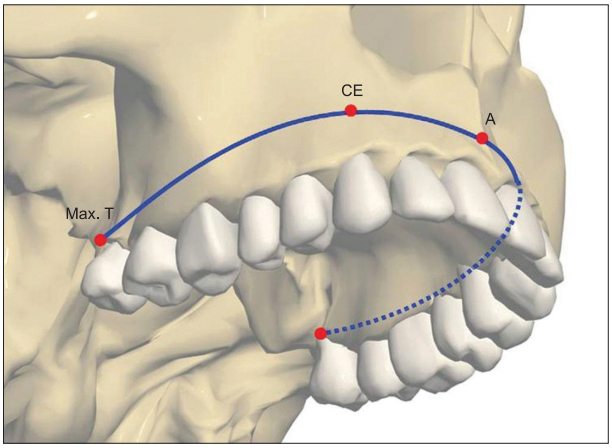

Figure 7. Maxillary basal curve length: Max. T, maxillary tuberosity; CE, canine eminence; A, A point.

Table 3. Comparison of three-dimensional maxillary and mandibular measurements between right and left sides (n = 38)

Variable	Total	Left side	Right side	*p*-value*
Mx height (mm)	49.63±3.78	49.52±3.77	49.75±3.85	0.29
Mx basal curve length (mm)	60.54±7.31	60.65±7.53	60.42±7.25	0.77
Mn body length (mm)	87.98±4.98	87.88±5.03	88.09±4.99	0.48
Mn basal curve length (mm)	98.19±5.98	97.74±5.29	98.63±6.65	0.22
MBC angle (°)	133.25±4.35	133.61±4.51	132.90±4.22	0.25
Ant Mn basal length (mm)	16.79±3.15	16.84±2.93	16.74±3.40	0.78
Post Mn basal length (mm)	75.62±5.02	75.42±4.94	75.82±5.16	0.29
Ramal length (mm)	57.57±5.82	57.54±5.89	57.60±5.82	0.78
Ramal mediolateral inclination (°)	84.61±3.25	84.37±3.17	84.85±3.35	0.44
Ramal anteroposterior inclination (°)	86.53±2.92	86.81±3.06	86.23±2.77	0.28
Gonial angle (°)	115.46±3.96	115.25±3.96	115.67±4.01	0.29
Gonion to midsagittal plane (mm)	48.38±3.60	48.22±3.80	48.54±3.43	0.56
Cond to midsagittal plane (mm)	52.38±3.35	52.01±3.29	52.75±3.44	0.08
Cond anteroposterior inclination (°)	66.55±8.20	66.33±4.42	67.37±5.15	0.07
Cond height (mm)	19.04±2.40	19.22±2.36	18.86±2.47	0.21
Cond width (mm)	17.64±2.68	17.28±2.50	18.01±2.83	0.07

Values are presented as mean ± standard deviation.
Mx, Maxillary; Mn, mandibular; MBC, mandibular body curve; Ant, anterior; Post, posterior; Cond, condyle.
*Paired t-test.

 http://dx.doi.org/10.4041/kjod.2013.43.2.62

Table 4. Comparison of three-dimensional measurements between male and female subjects

Variable	Total	Male (n = 18)	Female (n = 20)	*p*-value*
Sagittal				
SNA (°)	81.84 ± 2.53	81.92 ± 2.78	81.80 ± 2.37	NS
SNB (°)	79.83 ± 2.80	80.43 ± 2.63	79.28 ± 2.89	NS
ANB (°)	2.09 ± 1.25	1.68 ± 1.07	2.46 ± 1.30	NS
SNPg angle (°)	80.51 ± 3.13	81.46 ± 2.85	79.65 ± 3.19	NS
Facial angle (°)	90.40 ± 2.31	90.01 ± 2.21	90.76 ± 2.39	NS
A to N-Pg (mm)	1.52 ± 1.28	1.11 ± 1.22	1.88 ± 1.26	NS
Pg to NB (mm)	1.56 ± 1.06	1.89 ± 1.26	1.23 ± 0.71	NS
Angle of convexity (°)	2.94 ± 1.88	2.48 ± 2.03	3.46 ± 1.61	NS
Mx length (mm)	46.83 ± 3.00	47.98 ± 2.73	45.80 ± 2.92	0.02†
Mn body length (Me-Go) (mm)	87.98 ± 4.98	91.02 ± 3.07	85.25 ± 4.80	<0.001§
Ramal anteroposterior inclination (°)	86.53 ± 2.92	86.19 ± 2.44	86.84 ± 3.30	NS
Cond anteroposterior inclination (°)	67.29 ± 5.12	67.61 ± 5.49	66.99 ± 4.81	NS
Vertical				
Ant facial height (mm)	121.04 ± 6.87	125.12 ± 6.14	117.36 ± 5.31	<0.001‡
Upper facial height (mm)	54.13 ± 3.51	55.85 ± 2.38	52.58 ± 3.69	0.003‡
Lower facial height (mm)	67.72 ± 5.21	69.96 ± 5.65	65.71 ± 3.91	0.010‡
Mx height (mm)	49.63 ± 3.78	52.03 ± 2.74	47.47 ± 3.27	<0.001§
Ramal length (mm)	57.57 ± 5.82	61.21 ± 5.21	54.22 ± 4.10	<0.001§
Cond height (mm)	19.04 ± 2.40	19.47 ± 2.68	18.65 ± 2.09	NS
Y-Axis (°)	60.27 ± 2.69	59.99 ± 2.97	60.52 ± 2.46	NS
Gonial angle (°)	115.46 ± 3.96	113.77 ± 3.26	117.02 ± 3.95	<0.001§
Transverse				
Upper facial width (mm)	95.85 ± 4.68	98.98 ± 3.51	93.04 ± 3.74	<0.001§
Ant Mx basal width (mm)	33.17 ± 2.60	34.79 ± 2.29	31.71 ± 1.93	<0.001§
Post Mx basal width (mm)	65.35 ± 4.21	66.83 ± 4.32	64.02 ± 3.73	0.040†
Me angle (°)	66.91 ± 4.74	67.09 ± 3.47	66.75 ± 5.74	NS
Me deviation angle (°)	0.80 ± 0.83	0.83 ± 0.87	0.78 ± 0.81	NS
Menton to midline (mm)	0.92 ± 0.94	0.99 ± 1.02	0.86 ± 0.88	NS
Ramal mediolateral inclination (°)	84.61 ± 3.25	85.30 ± 2.19	83.97 ± 3.91	NS
Go to midsagittal (mm)	48.38 ± 3.60	50.24 ± 3.05	46.70 ± 3.24	<0.001§
Cond to midsagittal (mm)	52.38 ± 3.35	53.11 ± 2.71	51.73 ± 3.75	NS
Cond width (mm)	17.77 ± 2.60	18.35 ± 2.84	17.22 ± 2.25	NS
Other				
Mx basal curve length (mm)	61.19 ± 6.78	61.27 ± 8.19	61.10 ± 5.20	NS
Mn basal curve length (mm)	98.19 ± 5.98	102.31 ± 4.36	94.52 ± 4.73	<0.001§
MBC angle (°)	133.25 ± 4.35	132.44 ± 4.54	133.99 ± 4.10	NS
Ant Mn basal length (mm)	16.79 ± 3.15	18.02 ± 2.99	15.68 ± 2.90	0.001‡
Post Mn basal length (mm)	75.62 ± 5.02	77.85 ± 4.14	73.61 ± 4.94	<0.001§

Values are presented as mean ± standard deviation.
SNA, Sella-nasion-A point; SNB, sella-nasion-B point; ANB, A point-nasion-B point; SNPg, sella-nasion-pogonion; A, A point; N-Pg, nasion-pogonion; Pg, pogonion; NB, nasion-B point; Mx, maxillary; Mn, mandibular; Go, gonion; Me, menton; Cond, condylar; Ant, anterior; Post, posterior; MBC, mandibular body curve; NS, not significant.
*Independent t-test; †$p < 0.05$; ‡$p < 0.01$; §$p < 0.001$.
n is doubled in case of paired variables.

http://dx.doi.org/10.4041/kjod.2013.43.2.62

length of the curve of the basal arch of the maxilla by incorporating the A point, right and left canine eminence, and maxillary tuberosity, where *a* and *b* in the equation are the values of X coordinates of A point and maxillary tuberosity, respectively (Figure 7).

Statistical analysis

Statistical evaluation was performed using SPSS software ver. 16.0 (SPSS Inc., Chicago, IL, USA). Normal distribution of the parameters was assessed by the Kolmogorov-Smirnov test. Right and left variables were compared by a paired t-test. Gender dimorphism was evaluated by an independent samples t-test. Correlations among skeletal and dentoalveolar measurements were calculated by means of Pearson's correlation coefficient. To assess the reliability of the digitizing process, 10 CBCT scans were redigitized by the same operator, 2 weeks later. The intraclass correlation coefficient (ICC) between the duplicate measurements showed high reliability (ICC ranged between 0.997 and 0.931).

RESULTS

There were no significant differences in skeletal and dentoalveolar variables between right and left sides. Therefore, the values of both sides were combined before further analysis (Table 3).

There were no significant differences in the variables that assess the sagittal relationship between the cranial base, maxilla, and mandible between male and female subjects. However, all vertical dimension variables and some transverse variables - upper facial width ($p < 0.001$), anterior and posterior maxillary basal width ($p < 0.001$, $p = 0.04$, respectively), and Go-to-midsagittal

Table 5. Correlation between facial height variables and sagittal, vertical, transverse, and other three dimensional variables

Variable	Ant facial height (n = 38)	Upper facial height (n = 38)	Lower facial height (n = 38)
Sagittal			
SNA (n = 38)	−0.26 (0.12)	−0.16 (0.33)	−0.24 (0.15)
SNB (n = 38)	−0.13 (0.43)	0.004 (0.98)	−0.21 (0.21)
Mx length (n = 38)	0.45 (0.005)	0.41(0.01)	0.33 (0.04)
Mn body length (n = 76)	0.56 (<0.001)	0.56 (<0.001)	0.34 (0.04)
Vertical			
Upper facial height (n = 38)	0.69 (<0.001)		
Lower facial height (n = 38)	0.86 (<0.001)	0.23 (0.17)	
Mx height (n = 76)	0.85 (<0.001)	0.61 (<0.001)	0.70 (<0.001)
Ramal length (n = 76)	0.68 (<0.001)	0.49 (0.002)	0.57 (<0.001)
Gonial angle (n = 76)	−0.27 (0.11)	−0.35 (0.04)	−0.11 (0.50)
Transverse			
Upper facial width (n = 38)	0.71 (<0.001)	0.56 (0.001)	0.58 (<0.001)
Ant Mx basal width (n = 38)	0.51 (0.001)	0.37 (0.02)	0.42 (0.009)
Post Mx basal width (n = 38)	0.43 (0.007)	0.30 (0.07)	0.37 (0.02)
Go to midsagittal (n = 76)	0.65 (<0.001)	0.51 (0.001)	0.51 (0.001)
Cond to midsagittal (n = 76)	0.49 (0.002)	0.52 (0.001)	0.29 (0.08)
Other			
Mx basal curve length (n = 76)	0.12 (0.59)	0.11 (0.62)	0.10 (0.67)
Mn basal curve length (n = 76)	0.69 (<0.001)	0.63 (<0.001)	0.47 (0.005)
Ant Mn basal length (n = 76)	0.24 (0.15)	0.17 (0.32)	0.17 (0.31)
Post Mn basal length (n = 76)	0.44 (0.005)	0.48 (0.002)	0.24 (0.14)

Values are presented as *r* (*p*–value).
Pearson correlation.
SNA, Sella-nasion-A point; SNB, sella-nasion-B point; Mx, maxillary; Mn, mandibular; Ant, anterior; Post, posterior; Go, gonion; Cond, condylar.

 http://dx.doi.org/10.4041/kjod.2013.43.2.62

Table 6. Correlation among skeletal variables

Variable	Upper facial width (n = 38)	Mx length (n = 38)	Mx curve length (n = 76)	Me angle (n = 38)	MBC angle (n = 76)	Mn body length (n = 76)	Mn curve length (n = 76)	Gonial angle (n = 76)	Go to midsagittal (n = 76)	Ramal length (n = 76)	Ramal medio lateral inclination (n = 76)
Go to midsagittal (n = 76)		0.44 (0.006)	0.26 (0.24)	0.61 (<0.001)							
Cond to midsagittal (n = 76)		0.29 (0.08)	0.15 (0.50)	–0.01 (0.95)					0.44 (0.006)	0.11 (0.51)	0.48 (0.003)
Ramal length (n = 76)	0.66 (<0.001)			0.48 (0.003)		0.21 (0.22)	0.2 (0.02)	–0.62 (<0.001)	0.65 (<0.001)		
Ramal mediolateral inclination (n = 76)				0.53 (0.001)				–0.49 (0.002)	0.39 (0.02)	0.54 (0.001)	
Ramal anteroposterior inclination (n = 76)				–0.36 (0.03)		0.13 (0.44)	0.06 (0.72)	0.12 (0.47)	–0.22 (0.19)	–0.14 (0.42)	0.01 (0.96)
Mn body length (n = 76)	0.56 (<0.001)	0.48 (0.002)	0.18 (0.40)	–0.41 (0.01)	–0.15 (0.36)			–0.28 (0.10)			
Mn curve length (n = 76)	0.73 (<0.001)	0.51 (0.002)	0.25 (0.29)	–0.12 (0.51)	–0.12 (0.51)	0.91 (<0.001)		–0.45 (0.008)			
Ant Mn basal length (n = 76)	0.26 (0.12)	0.20 (0.23)	0.01 (0.97)	–0.13 (0.43)	0.13 (0.44)	0.36 (0.03)	0.44 (0.009)				
Post Mn basal length (n = 76)	0.45 (0.004)	0.44 (0.06)	0.26 (0.24)	–0.39 (0.02)	–0.36 (0.03)	0.86 (<0.001)	0.73 (<0.001)	–0.20 (0.24)			
Mx height (n = 76)	0.65 (<0.001)	0.39 (0.02)	–0.001 (0.99)			0.66 (<0.001)	0.74 (<0.001)		0.60 (<0.001)	0.60 (<0.001)	
Ant Mx basal width (n = 38)		0.38 (0.02)	0.25 (0.24)								
Post Mx basal width (n = 38)		0.20 (0.23)	0.05 (0.82)								
Upper facial width (n = 38)		0.62 (<0.001)	0.23 (0.30)								

Values are presented as *r* (*p*-value).
Pearson correlation.
Go, Gonion; Cond, condyle; Mn, mandibular; Ant, anterior; Post, posterior; Mx, maxillary; MBC, mandibular body curve.

($p < 0.001$) - were significantly different according to gender. Nevertheless, such differences were absent in both condylar width and the condyle-to-midsagittal dimensions.

The basal curve of the mandible showed a longer curve length in male subjects (102.31 mm) than in female subjects (94.52 mm) ($p < 0.001$), but there was no significant difference in the maxillary basal curve length (61.19 mm) (Table 4).

Table 5 shows the correlations among facial heights and several skeletal and dentoalveolar variables. The anterior, upper, and lower facial heights had strong to moderate correlations[15] with upper facial width (r = 0.71, 0.56, and 0.58, respectively), the Go-to-midsagittal measurement (r = 0.65, 0.51, and 0.51, respectively), and MBC length (r = 0.69, 0.63, and 0.47, respectively). Moreover, the 3 facial heights showed moderate-to-weak correlations with maxillary length (r = 0.45, 0.41, and 0.33, respectively) and anterior maxillary basal width (r = 0.51, 0.37, and 0.42, respectively), but there were no significant correlations with the maxillary basal curve length or the anterior mandibular body length.

Regarding the correlations among other skeletal variables, the upper facial width had significant moderate correlations with ramal length, mandibular basal curve length, and maxillary height and length (r = 0.66, 0.73, 0.65, and 0.62, respectively). The maxillary length had moderate correlations with mandibular basal curve length and Go-to-midsagittal measurement (r = 0.51, and 0.44, respectively). In addition, the ramal length demonstrated a significant moderate correlation with the Me angle and a negative correlation with the gonial angle (r = 0.48 and –0.62, respectively) (Table 6).

The relationship between the condylar and ramal variables is shown in Table 7. The condylar height was correlated with the ramal mediolateral (r = 0.38), but not with the anteroposterior, inclination. However, it correlated with the condylar anteroposterior inclination (r = 0.48), and the condylar inclination had a weak negative correlation with the gonial angle (r = –0.33).

DISCUSSION

The 3D evaluation of cephalometric variables assists clinicians in obtaining enhanced diagnosis and in treatment planning. Traditionally, 2D cephalometric analyses suffer from inherent drawbacks related to the 2D technique, which may have led to errors in their norms. Therefore, 3D analysis may represent the key to overcoming these weaknesses.

Cheung et al.[14] evaluated the mandibular body length from Me to Antegonion and from Me to Go. However, they overlooked the assessment of the curved nature of the mandible and maxilla. Lee et al.[16] proposed the MBC point and reported a significant difference between the asymmetric and normal occlusion groups in the posterior mandibular body length, but this difference was not significant in the mandibular body length (Me–Go).

In our study, a new approach was applied to evaluate the curve length of the mandibular body by calculating the length of the curve passing through Me, MBC, and Go to achieve a more accurate representation of the length of the mandibular body instead of using an approximation of the curve with a line. The maxillary and mandibular curve lengths might guide clinicians in treatment planning by shedding light on the limits of the basal arches that enclose the teeth. In addition, it might be useful to use the 2 equations of the curves for arch coordination. Therefore, the 3D analysis of CBCT images requires deeper understanding of mathematics, spatial geometry, trigonometry, and algebra.

Previous 2D evaluations of the Korean cephalometric norms have been conducted.[17] Although the angular values in those evaluations were close to ours, the linear measurements were different. The mandibular body length was 78.5 mm in male subjects in that 2D study, but 91 mm in ours. This difference was because the previous definition of the mandibular body length (Me–Go) became deficient when applied in 3D. In addition, the ramal height of male subjects in the Lee's[17] study was 56.8 mm, whereas in ours, it was 61.2 mm. This might be because it was measured from the articulare

Table 7. Correlations between condylar and ramal variables

Variable	Gonial angle	Cond to midsagittal	Ramal length	Ramal mediolateral inclination	Ramal anteroposterior inclination	Cond anteroposterior inclination
Cond anteroposterior inclination	–0.33 (0.04)	–0.32 (0.05)	0.15 (0.39)	0.38 (0.02)	0.19 (0.27)	
Cond height		–0.30 (0.07)	0.18 (0.29)	0.38 (0.02)	0.08 (0.64)	0.48 (0.003)
Cond width		0.66 (<0.001)				–0.10 (0.54)

Pearson correlation. Data is presented as r (p-value).
Cond, Condyle.

 http://dx.doi.org/10.4041/kjod.2013.43.2.62

in the 2D study, but in ours it was measured from the condylion. This was due to the nature of the 3D image, in which there is no intersection between the cranial base and the ramus.

A previous study using 3D analysis reported normal values of selected cephalometric variables, but no attempt was made to evaluate the relationships among these variables.[14] In our study, significant strong-to-moderate correlations of facial heights were noticed with several transverse variables, such as upper facial width and Go-to-midsagittal measurement as shown in Table 5. Moreover, the upper facial width had strong-to-moderate correlations with the maxillary height and length and MBC length. These findings may suggest the existence of relationships among facial dimensions in the normal-occlusion sample.

Regarding the condyle, You et al.[18] suggested that the condylar unit, consisting of condyle, condylar neck, and part of the ramus, plays a central role in mandibular asymmetry, whereas Huntjens et al.[19] found condylar asymmetries did not correlate well with facial asymmetry. In our study, the reported correlation between the condylar and mandibular variables might be attributed to the adaptive capacity of the condyle, as suggested by Enlow and Hans.[20] For example, in Table 7, the negative correlation between the condylar anteroposterior inclination and the gonial angle tends to preserve the proportion between the height of the mandible and its sagittal position in the normal occlusion population.

Recently, the difference in ramal length from one side to the other was reported as a characteristic of both mandibular-retrusion and prognathism groups.[21] In Table 6, the ramal length demonstrated a significant moderate negative correlation with the gonial angle (r = –0.62). This means that the longer the ramus, the smaller its angle with the mandibular body. This configuration can be a way to prevent elongation of facial height, but a deviation on one side from this relationship may result in facial asymmetry.

In our results, there was no significant difference between the right and left sides. However, Shah and Joshi[22] reported asymmetry in the normal occlusion population with pleasing facial features. This discrepancy might be the result of difficulties in landmark identification in their study, due to superimposition of anatomical structures.

In our study, the comparison between male and female subjects showed significant differences in several vertical and transverse measurements, but there were no significant differences in the sagittal dimensions. These results were in agreement with Thilander et al.,[23] who reported that the linear craniofacial measurements were larger in male subjects than in female subjects, while angular measurements showed no statistical differences. This might suggest that the dimensions of the face played a major role in the gender dimorphism.

In a comparison of our data with the data obtained by Cheung et al.[14] study, facial height and lower facial height were larger in the Korean group than in the Chinese, whereas the upper facial height was smaller in Koreans. This can be attributed to ethnic differences and the different landmarks. In addition, the facial angle (Frankfort to nasion-pogonion angle) in Koreans was larger than that of the southern Chinese population (90° vs. 86.7°, respectively), implying a more protrusive chin in our sample. Meanwhile, SNA (sella-nasion-A point) and SNB (sella-nasion-B point) were more protrusive in the Chinese population (84.9° vs. 81.4°, respectively).

We limited our subject base to young adults to eliminate the effect of growth, because changes in facial features by age have been reported.[23,24] In addition, our method used for digitization of the CBCT images might be technique sensitive. Further studies are recommended to evaluate the operator learning curve, the reliability of the measurements, the predictors of the correlated variables, and the norms for different ethnic groups.

CONCLUSION

This study has assessed new measurements and evaluated the relationships among skeletal and dentoalveolar variables obtained through 3D cephalometric analysis in a normal occlusion sample. The normative values of new 3D cephalometric parameters, including the maxillary and mandibular curve length, were obtained. Strong-to-moderate correlation values were shown between several vertical and transverse measurements, indicating the existence of relationships between different facial dimensions in a normal occlusion group. This result can be useful for accurate diagnosis and treatment planning and for evaluation of treatment outcomes of orthodontics or orthognathic surgery.

REFERENCES

1. Baumrind S, Frantz RC. The reliability of head film measurements. 1. Landmark identification. Am J Orthod 1971;60:111-27.
2. Ahlqvist J, Eliasson S, Welander U. The cephalometric projection. Part II. Principles of image distortion in cephalography. Dentomaxillofac Radiol 1983;12:101-8.
3. Kusnoto B, Evans CA, BeGole EA, de Rijk W. Assessment of 3-dimensional computer-generated cephalometric measurements. Am J Orthod Dentofacial Orthop 1999;116:390-9.
4. Rousset MM, Simonek F, Dubus JP. A method for correction of radiographic errors in serial three-

http://dx.doi.org/10.4041/kjod.2013.43.2.62

dimensional cephalometry. Dentomaxillofac Radiol 2003;32:50-9.
5. Nakasima A, Terajima M, Mori N, Hoshino Y, Tokumori K, Aoki Y, et al. Three-dimensional computer-generated head model reconstructed from cephalograms, facial photographs, and dental cast models. Am J Orthod Dentofacial Orthop 2005; 127:282-92.
6. Ludlow JB, Gubler M, Cevidanes L, Mol A. Precision of cephalometric landmark identification: cone-beam computed tomography vs conventional cephalometric views. Am J Orthod Dentofacial Orthop 2009;136:312.e1-10.
7. Ludlow JB, Laster WS, See M, Bailey LJ, Hershey HG. Accuracy of measurements of mandibular anatomy in cone beam computed tomography images. Oral Surg Oral Med Oral Pathol Oral Radiol Endod 2007; 103:534-42.
8. Cevidanes LH, Bailey LJ, Tucker GR Jr, Styner MA, Mol A, Phillips CL, et al. Superimposition of 3D cone-beam CT models of orthognathic surgery patients. Dentomaxillofac Radiol 2005;34:369-75.
9. Cevidanes LH, Bailey LJ, Tucker SF, Styner MA, Mol A, Phillips CL, et al. Three-dimensional cone-beam computed tomography for assessment of mandibular changes after orthognathic surgery. Am J Orthod Dentofacial Orthop 2007;131:44-50.
10. van Vlijmen OJ, Maal TJ, Bergé SJ, Bronkhorst EM, Katsaros C, Kuijpers-Jagtman AM. A comparison between two-dimensional and three-dimensional cephalometry on frontal radiographs and on cone beam computed tomography scans of human skulls. Eur J Oral Sci 2009;117:300-5.
11. van Vlijmen OJ, Bergé SJ, Bronkhorst EM, Swennen GR, Katsaros C, Kuijpers-Jagtman AM. A comparison of frontal radiographs obtained from cone beam CT scans and conventional frontal radiographs of human skulls. Int J Oral Maxillofac Surg 2009;38: 773-8.
12. Gribel BF, Gribel MN, Manzi FR, Brooks SL, McNamara JA Jr. From 2D to 3D: an algorithm to derive normal values for 3-dimensional computerized assessment. Angle Orthod 2011;81:3-10.
13. Farronato G, Garagiola U, Dominici A, Periti G, de Nardi S, Carletti V, et al. "Ten-point" 3D cephalometric analysis using low-dosage cone beam computed tomography. Prog Orthod 2010;11:2-12.
14. Cheung LK, Chan YM, Jayaratne YS, Lo J. Three-dimensional cephalometric norms of Chinese adults in Hong Kong with balanced facial profile. Oral Surg Oral Med Oral Pathol Oral Radiol Endod 2011; 112:e56-73.
15. Ratner B. Statistical modeling and analysis for database marketing: effective techniques for mining big data. Boca Raton: Chapman and Hall/CRC; 2003. p. 17.
16. Lee H, Bayome M, Kim SH, Kim KB, Behrents RG, Kook YA. Mandibular dimensions of subjects with asymmetric skeletal Class III malocclusion and normal occlusion compared with cone-beam computed tomography. Am J Orthod Dentofacial Orthop 2012;142:179-85.
17. Lee CT. Standards for Korean adult facial relationships by various roentgeno-cephalometric analysis. Korean J Orthod 1988;18:459-74.
18. You KH, Lee KJ, Lee SH, Baik HS. Three-dimensional computed tomography analysis of mandibular morphology in patients with facial asymmetry and mandibular prognathism. Am J Orthod Dentofacial Orthop 2010;138:540.
19. Huntjens E, Kiss G, Wouters C, Carels C. Condylar asymmetry in children with juvenile idiopathic arthritis assessed by cone-beam computed tomography. Eur J Orthod 2008;30:545-51.
20. Enlow DH, Hans MG. Essentials of facial growth. Philadelphia: W.B. Saunders; 1996. p. 72.
21. Kim EJ, Palomo JM, Kim SS, Lim HJ, Lee KM, Hwang HS. Maxillofacial characteristics affecting chin deviation between mandibular retrusion and prognathism patients. Angle Orthod 2011;81:988-93.
22. Shah SM, Joshi MR. An assessment of asymmetry in the normal craniofacial complex. Angle Orthod 1978;48:141-8.
23. Thilander B, Persson M, Adolfsson U. Roentgen-cephalometric standards for a Swedish population. A longitudinal study between the ages of 5 and 31 years. Eur J Orthod 2005;27:370-89.
24. Shaw RB Jr, Kahn DM. Aging of the midface bony elements: a three-dimensional computed tomographic study. Plast Reconstr Surg 2007;119:675-81.

 http://dx.doi.org/10.4041/kjod.2013.43.2.62